Physicochem. Probl. Miner. Process., 61(4), 2025, 208680

http://www.journalssystem.com/ppmp

Physicochemical Problems of Mineral Processing

ISSN 1643-1049

Chelation-driven selective adsorption of methyl-enhanced hydroxamic acid for high-efficiency ilmenite/clinochlore flotation separation

Fusheng Niu [1,2], Jingtao Liu [1], Zehong Cheng [1,3], Jinxia Zhang [1,2], Yuying Chen [1]

[1] College of Mining Engineering, North China University of Science and Technology, Tangshan 063210, China

[2] Collaborative Innovation Center of Green Development and Ecological Restoration of Mineral Resources, Tangshan 063210, China

[3] State Environmental Protection Key Laboratory of Mineral Metallurgical Resources Utilization and Pollution Control, Wuhan University of Science and Technology, Wuhan 430081, China

Corresponding authors: chengzehong@ncst.edu.cn (Zehong Cheng), kyky@ncst.edu.cn (Jinxia Zhang)

Abstract: To address the issue of clinochlore and other gangue minerals easily reporting to the concentrate during ilmenite flotation, thereby reducing concentrate quality, this study synthesized p-methylbenzohydroxamic acid (MBHA) using p-methylbenzoic acid as the raw material. The compound was characterized by FTIR and ^{1}H NMR spectroscopy and subsequently applied to ilmenite flotation. Artificial mixed ore flotation tests demonstrated that under conditions of pH 7.0 and MBHA dosage of 300 mg/L, the ilmenite recovery reached 84.26% with a TiO_2 grade of 43.36% in the concentrate. Contact angle and adsorption analyses reveal that at an MBHA dosage of 300 mg/L, the adsorption capacity reaches 0.046 mg·g^{-1}, indicating MBHA adsorption on ilmenite surfaces, while the surface contact angle increases from 43.60° to 80.00°, demonstrating enhanced hydrophobicity. FTIR and XPS analyses confirmed strong chemisorption via "O–M–O" five-membered chelation with Fe^{3+}/Ti^{4+} on ilmenite, while weak physical adsorption dominated on clinochlore. Zeta potential measurements showed significant negative shifts (up to -13.40 mV at pH 6.0–8.0) due to MBHA chemisorption on ilmenite. This work provides a theoretical foundation for efficient low-grade ilmenite separation.

Keywords: hydroxamic acid, ilmenite, clinochlore, flotation mechanism, flotation collector

1. Introduction

Titanium, as a critical strategic metal, plays an irreplaceable role in aerospace manufacturing, advanced military technology, biomedical engineering, and green energy transition due to its exceptional mechanical strength, environmental resistance, and thermochemical stability(Hong et al., 2025; Zhang et al., 2011). However, China's titanium resource utilization faces critical challenges: Primary ilmenite deposits in regions like Panxi exhibit "lean, fine-grained, and complexly intergrown" characteristics, where gangue minerals (e.g., clinochlore) resist efficient separation (Zhao et al., 2025). Current beneficiation technologies demonstrate systemic inefficiencies when processing such low-grade (TiO_2 content <10%), ultrafine (micrometer-scale) ores, resulting in severe metal loss and persistent reliance on imported high-grade titanium concentrates (typically >48% TiO_2) (Zhu et al., 2011). This technological gap underscores the strategic necessity of developing advanced mineral processing solutions for low-grade primary ilmenite resources, which is critical for safeguarding China's titanium industry sovereignty and underpinning national strategic industries. (Fan et al., 2008; Mehdilo et al., 2015).

Flotation represents an effective approach to achieving the resource utilization and large-scale utilization of ilmenite, and enhancing the performance of collectors is the key to realizing efficient flotation separation of ilmenite (Peng et al., 2024). Current ilmenite collectors primarily include fatty acids, hydroxamates, organic phosphonic acids, and arsenics (Qi et al., 2025; Yu et al., 2025b). While fatty acid collectors dominate oxide mineral flotation due to low cost and availability, their poor selectivity in ilmenite systems stems from overlapping surface properties between ilmenite and associated gangue minerals (Yu et al., 2025a). Phosphonic acid collectors demonstrate enhanced

DOI: 10.37190/ppmp/208680

ilmenite selectivity with reduced toxicity compared to fatty acids, yet their industrial adoption remains constrained by prohibitive synthesis costs (Bai et al., 2025; Cheng et al., 2025). Arsenic-based collectors face operational limitations from complex synthesis routes and acute toxicity. Hydroxamic acids emerge as superior alternatives through their unique chelation mechanism: Nonpolar groups form stable five-membered "O–M–O" and four-membered "N–M–O" chelates with metallic ions (Pb^{2+}, Co^{2+}, Ti^{4+}, La^{3+}, Ta^{5+}), achieving exceptional selectivity (Liu et al., 2025a; Liu et al., 2025b). Coupled with low toxicity and strong collecting power, these characteristics drive hydroxamates' widespread application in ilmenite flotation systems.

In recent years, a series of hydroxamic acids have been developed and applied to the flotation of oxide minerals. Fang Shuai's team demonstrated that Pb-BHA composite collectors exhibit synergistic effects superior to standalone Pb-BHA applications through enhanced interparticle bridging (Fang et al., 2018). Xiao Wei's mechanistic study revealed aluminum ions (Al^{3+}) activate ilmenite surfaces by forming stable Fe-O-Al-BHA and Ti-O-Al-BHA ternary chelate complexes when using BHA with terpineol frother (Xiao et al., 2022). Concurrently, Zhao Gang's work with cyclohexyl hydroxamic acid identified exceptional calcium-binding affinity through Ca^{2+}-centered coordination architectures in scheelite flotation (Zhao et al., 2013). These breakthroughs collectively demonstrate that strategic functional group modifications - particularly through metal ion complexation and alkyl chain optimization - fundamentally govern hydroxamates' collector efficacy, establishing molecular engineering as a critical pathway for next-generation flotation reagent development.

Based on the surface properties of ilmenite, this study synthesized MBHA through esterification and hydroxamation reactions. Single mineral and artificial mixed ore flotation tests were conducted to investigate the collecting ability of MBHA on ilmenite and clinochlore, with comparisons to sodium oleate (NaOL). Analytical techniques including XPS, FT-IR, and TOC were employed to study the interaction mechanism between the collector MBHA and ilmenite.

2. Materials and methods

2.1. Materials

The pure mineral samples of ilmenite and clinochlore used in this experiment were obtained from a mining area in Hebei Province. Through a series of processes including ore crushing, grinding, magnetic separation, and repeated impurity removal using a shaking table, monomineral samples of ilmenite and clinochlore with particle sizes of -74 μm +38 μm were collected via wet sieving for flotation tests. A portion of the samples was further ground to approximately 5 μm for characterization experiments such as FT-IR, Zeta potential measurements, and XPS analysis. According to X-ray diffraction (XRD) patterns and chemical composition analysis results (Fig. 1 and Table 1), both ilmenite and clinochlore exhibited purity levels exceeding 90%, meeting the requirements for flotation experimentation.

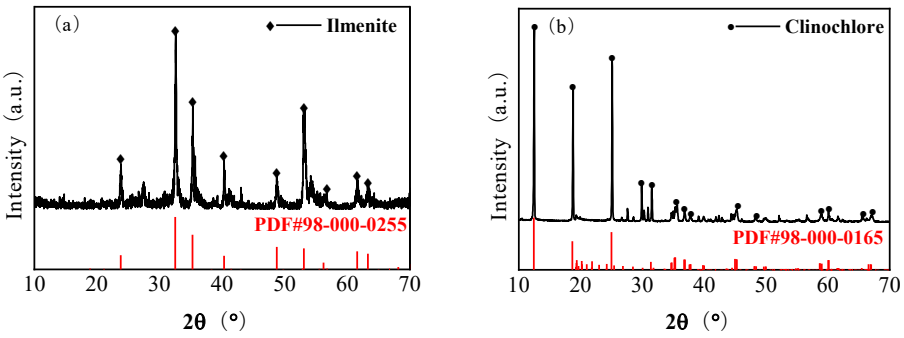

Fig. 1. X-ray diffraction patterns for ilmenite (a) and clinochlore (b)

Table 1. Chemical composition of ilmenite and clinochlore (mass fraction, %)

Samples	TiO_2	Fe_2O_3	FeO	MgO	CaO	Al_2O_3	SiO_2	MnO_2
Ilmenite	51.42	9.00	33.5	-	0.31	1.66	1.57	1.65
Clinochlore	0.20	6.29	-	31.39	2.82	11.48	38.07	0.064

2.2. Reagents

All chemicals used in the experiments, including p-toluic acid, hydroxylamine hydrochloride, methanol, concentrated sulfuric acid, hydrochloric acid, and sodium hydroxide, were provided by Shanghai Macklin Biochemical Technology Co., Ltd. Additionally, deionized water was employed in all tests.

The synthesis of MBHA was achieved through a two-step reaction sequence. The first step consisted of the synthesis of methyl p-toluate via an esterification reaction, followed by the second step involving hydroxamation of methyl p-toluate to afford the hydroxamic acid product.

The esterification reaction was conducted as follows: *p*-Toluic acid was charged into a 250 mL three-necked flask. The reaction system maintained a molar ratio of alcohol to acid at 4.5:1, with H_2SO_4 loading equivalent to 15 mol% relative to the acid. Methanol and concentrated H_2SO_4 were introduced sequentially. The mixture was heated to 65°C under controlled water-bath conditions and held isothermally for 6 h with vigorous magnetic stirring and reflux condensation. Upon completion, the crude product was neutralized with saturated aqueous Na_2CO_3 solution. Subsequent separatory extraction using a 250 mL separatory funnel afforded methyl *p*-toluate as the organic phase (Yadav and Katole, 2025).

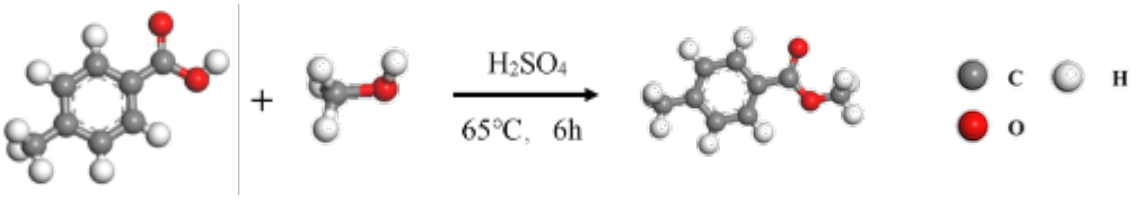

Fig. 2. Esterification reaction

The hydroximation procedure is illustrated in Fig. 3. Hydroxylamine hydrochloride and sodium hydroxide were separately dissolved in methanol. The sodium hydroxide solution was carefully added to the hydroxylamine hydrochloride solution, followed by 1 h of reaction and filtration to obtain the hydroxylamine solution. Methyl p-toluate was then added dropwise to the hydroxylamine solution, and the mixture was reacted at 50°C for 4 h. Hydrochloric acid (HCl) was introduced to crystallize the hydroxamic acid, which precipitated from the solution. Complete crystallization was achieved using a rotary evaporator (Zhang et al., 2022). The crude hydroxamic acid was recrystallized from acetic acid solution to obtain high-purity product. Characterization results are detailed in Section 3.1.

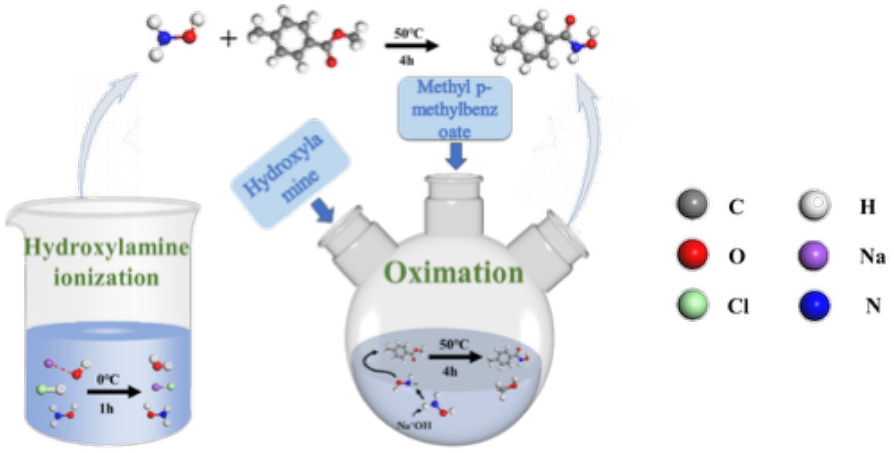

Fig. 3. Reaction mechanisms during the synthesis process of MBHA

2.3. Flotation experiment

Flotation experiments were conducted using an XFG-115 laboratory-scale hanging-trough flotation machine equipped with a 30 mL polymethyl methacrylate (PMMA) cell. For single-mineral flotation tests, dosage and pH condition experiments were performed, including comparative studies of MBHA

and NaOL. Specifically, 2.00 g of single mineral sample was mixed with 30 mL deionized water in the flotation cell at 2000 r/min for 3 min. The slurry pH was adjusted to target values using NaOH or HCl solutions under 2 min agitation. Subsequently, the collector was introduced and conditioned for 2 min, followed by a 5-min flotation process. Both froth product and tailings were collected, dried, and weighed. Detailed procedures are illustrated in Fig. 2. The single-mineral flotation recovery was calculated according to Equation (1).

$$\varepsilon = \frac{m_1}{m_1+m_2} \times 100\% \quad (1)$$

where ε represents the ilmenite recovery (%), and m1 and m2 are the masses (g) of the froth product and tailings, respectively.

In artificial mixed-mineral flotation tests, 2.00 g of blended minerals with a mass ratio of 1:1 between ilmenite and clinochlore were subjected to flotation. Subsequent procedures followed the single-mineral flotation protocol. The artificial mixed-mineral flotation recovery was calculated using Equation (2). All flotation tests were conducted in triplicate, with mean values reported as final results (errors < ±0.5%).

$$\varepsilon = \frac{\beta}{\alpha} \times \gamma \times 100\% \quad (2)$$

where ε denotes the ilmenite recovery (%), β represents the concentrate grade (%), α is the feed grade (%), and γ indicates the concentrate yield (%).

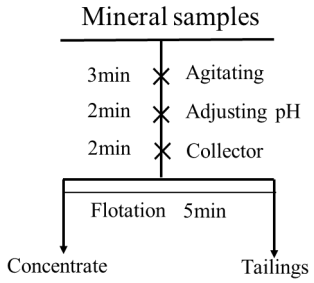

Fig. 4. Flotation Protocol

2.4. Contact angle measurements

Contact angle measurements of ilmenite and clinochlore before and after interaction with the MBHA collector were performed using a contact angle goniometer. The sample preparation protocol was as follows: 2.00 g of purified mineral particles (-38 μm) pre-washed with deionized water were sequentially treated with reagents according to the flotation test protocol. The slurry was stirred on a magnetic stirrer for 15 min, filtered, and the filter cake was dried in a vacuum oven at 30°C. The dried sample was compressed under high pressure in a tablet press to form compact and smooth-surfaced pellets for contact angle testing.

2.5. FI-TR measurements

FTIR spectra of ilmenite and clinochlore before and after interaction with the MBHA collector were analyzed using a Nicolet 740 FTIR spectrometer (Thermo Fisher Scientific, USA). The sample preparation protocol for infrared spectroscopy was as follows: 2.00 g of purified mineral particles were added to a beaker containing 30 mL of deionized water. Reagents were sequentially introduced into the suspension according to the flotation test conditions, followed by continuous agitation on a magnetic stirrer for 1 h to ensure sufficient reaction. The slurry was then filtered and rinsed three times with deionized water to remove residual reagents. The washed mineral samples were dried in a vacuum oven at 30°C. After complete drying, the samples were homogeneously mixed with potassium bromide (KBr) at a mass ratio of 1:100 in an agate mortar and pressed into transparent pellets for FTIR analysis.

2.6. Zeta potential measurements

Zeta potential measurements of mineral samples were conducted at room temperature using a Malvern Zetasizer (Nano-ZS90, Malvern Panalytical, UK). The experimental procedure was as follows: 20.00 mg

of purified mineral particles (<5 μm) were dispersed in 50 mL of 1×10−3 mol/L KCl aqueous solution or deionized water. Reagents were sequentially added according to flotation test conditions, and the pH was adjusted to predetermined values within 5 min using NaOH or HCl solutions. The suspension was stirred at a constant speed on a magnetic stirrer for 10 min, followed by a 5-min settling period to allow coarse particle sedimentation. Supernatant containing fine particles was carefully collected using a disposable pipette for zeta potential analysis. Each sample underwent three replicate measurements, and the final result was reported as the arithmetic mean.

2.7. Adsorption experiments

The total organic carbon (TOC) content in the supernatant was quantified using a TOC-L series analyzer equipped with an autosampler (Shimadzu Corporation, Japan). The analysis was performed on the supernatant obtained after interaction with reagents, where undetectable suspended solids were removed by centrifugation. The TOC measurement protocol was as follows: 2.00 g of purified mineral particles were added to a beaker containing deionized water. A predetermined volume of reagents was introduced to adjust the total solution volume to 30 mL. The suspension was agitated for 10 min using a magnetic stirrer and then centrifuged to separate solid-liquid phases. The clarified supernatant was retained for TOC analysis. Surface adsorption of reagents onto the minerals was calculated based on TOC depletion, using the following formula:

$$\Gamma = (C_0 - C_c) \cdot V/Q \tag{3}$$

where Γ is the adsorption capacity (mg/g), C_0 and C_e are the initial concentration and supernatant concentration (mg/L), V is the volume of the supernatant (L), and Q is the mass of the mineral sample (g).

2.8. XPS measurements

The changes in surface chemical environment of minerals before and after interaction with collectors were analyzed using an ESCALAB Xi+ spectrometer (Thermo Fisher Scientific, USA). The X-ray photoelectron spectroscopy (XPS) sample preparation method was as follows: 1.00 g mineral sample was mixed with 40 mL deionized water in a beaker, reagents were sequentially added according to the flotation procedure, stirred with a magnetic stirrer for 30 min. After the reagents completely reacted with the minerals, the minerals were washed with deionized water and filtered, dried in a vacuum oven at 40°C, and the dried sample was used for XPS analysis.

3. Results and discussion

3.1. Synthesis and characterization of MBHA

MBHA was characterized using Fourier transform infrared spectroscopy (FTIR) and ^{1}H nuclear magnetic resonance (^{1}H NMR), the infrared absorption peaks of various functional groups and molecular structure peaks in MBHA are shown in Fig. 5.

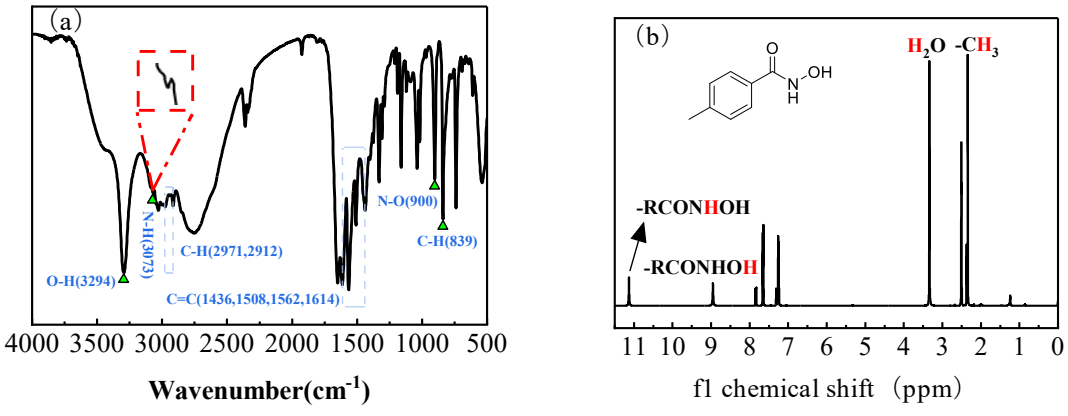

Fig. 5. (a) The FTIR spectrum of MBHA and (b) nuclear magnetic resonance hydrogen spectrum of MBHA

In the FT-IR spectrum Fig. 5(a) of MBHA, the absorption peaks at 3073 cm^{-1} and 3294 cm^{-1} correspond to the stretching vibrations of N-H and O-H, respectively (Liu et al., 2024). The peak at 1655 cm^{-1} is attributed to the stretching vibration of C=O. The absorption peaks at 1436 cm^{-1}, 1508 cm^{-1}, 1562 cm^{-1}, and 1614 cm^{-1} are characteristic of the benzene ring. The single shoulder absorption vibration peak at 1330 cm^{-1} corresponds to C-N, while the stretching vibration absorption peak of N-O (or C=N) appears at 900 cm^{-1} (Luo et al., 2024). The bands near 2912 cm^{-1} and 2971 cm^{-1} are assigned to the stretching vibrations of $-CH_3$ (Bai et al., 2025). The peak at 839 cm^{-1} corresponds to the stretching vibration of para-substituted benzene ring C-H. It can be seen that the characteristic peaks of the benzene ring, para-substituted methyl groups, and the C=O and N-H stretching vibration absorption peaks of hydroxamic acid are particularly prominent, leading to the inference that the target product MBHA was successfully synthesized.

In Fig. 5(b), the peaks at 8.94 ppm and 11.12 ppm correspond to the -RCONHOH in MBHA. The peak of the para-substituted methyl group in MBHA appears at 2.34 ppm, and the -OH peak of H_2O is observed at 3.33 ppm (Wang et al., 2023). The types and numbers of hydrogen atoms in the product are consistent with those of MBHA, leading to the inference that the target product MBHA was successfully synthesized.

3.2. Micro-flotation results

3.2.1. Flotation of single minerals

Sodium oleate is a compound composed of a hydrophobic group and a hydrophilic group, exhibiting excellent emulsification, penetration, and detergency properties, with good solubility in warm water. It is commonly used as an anionic surfactant and is widely applied in the flotation of oxidized ores in the mining industry, serving as a common collector for ilmenite. This section investigates the effect of pH on the flotation behavior of ilmenite and clinochlore through flotation tests with MBHA and NaOL dosages fixed at 200 mg/L. The results are shown in Fig. 6.

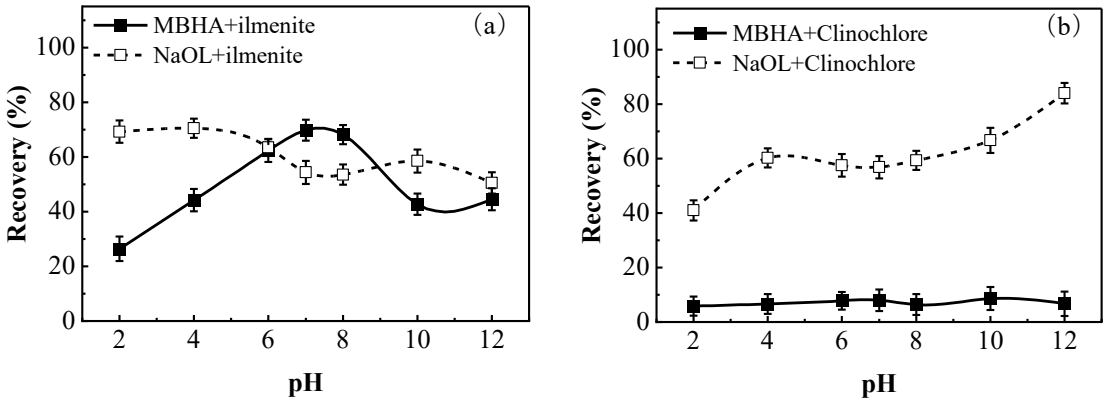

Fig. 6. The effect of pH on the flotation performance of (a) ilmenite and (b) clinochlore (the dosage of collector is 200 mg/L)

As shown in Fig. 6(a), when NaOL is used as the collector, the recovery of ilmenite in acidic conditions is higher than in neutral and alkaline environments. At pH=4.0, the recovery reaches 70.50%. When MBHA is employed as the collector, ilmenite exhibits excellent floatability in neutral, weakly acidic, and weakly alkaline conditions, with the highest recovery of 69.80% achieved at pH=7.0. This is because hydroxamic acid ions and hydroxamic acid molecules coexist at comparable concentrations in the aqueous solution within the pH range of 5.0–9.0, resulting in strong collecting capability (Kuixin et al., 2023). According to Fig. 6(b), when NaOL is used as the collector, the recovery of clinochlore increases with rising pH, attaining higher values in alkaline and neutral environments. In contrast, when MBHA is applied as the collector, the recovery of clinochlore shows minimal variation with pH changes.

Under their respective optimal pH conditions, the effects of MBHA and NaOL dosages on the flotation behavior of ilmenite and clinochlore were investigated. The results are shown in Fig. 7.

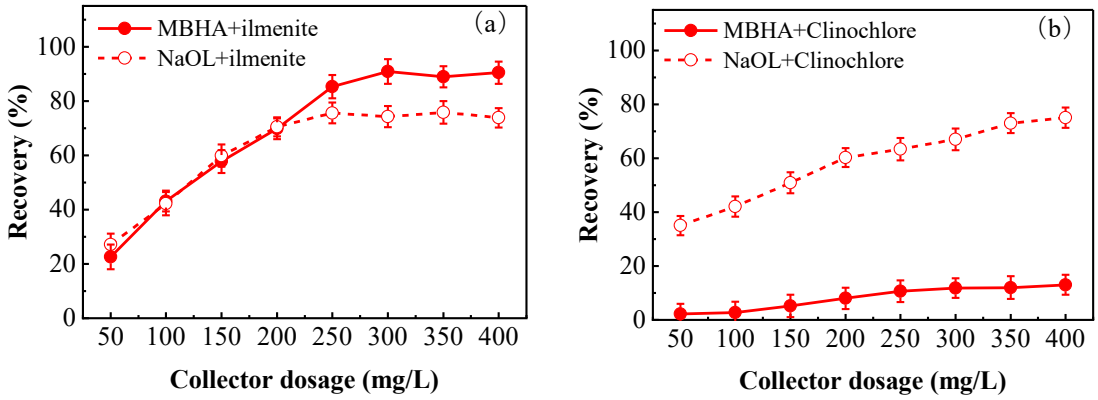

Fig. 7. The effect of collector dosages of 50 to 400 mg/L on the flotation performance of (a) ilmenite and (b) clinochlore (MBHA: pH 7.0, NaOL: pH 4.0)

As shown in Fig. 7(a), when NaOL is used as the collector, the recovery of ilmenite increases with higher collector dosage. When the NaOL dosage exceeds 250 mg/L, the recovery of ilmenite shows almost no further increase. When MBHA is empoyed as the collector, the recovery reaches 85.30% at a dosage of 250 mg/L. Further increases in MBHA dosage result in minimal changes to ilmenite recovery, which stabilizes. As illustrated in Fig. 7(b), the recovery of clinochlore demonstrates an upward trend when NaOL serves as the collector. In contrast, when MBHA is applied as the collector, clinochlore recovery exhibits negligible variation with increasing MBHA dosage, reaching a maximum of only 11.80% at 300 mg/L.

The single mineral flotation test results indicate that NaOL exhibits a certain collecting effect on both ilmenite and clinochlore but demonstrates poor selectivity, while MBHA shows excellent collecting performance for ilmenite and almost no collection of clinochlore, exhibiting good selectivity, and is a highly promising collector for the flotation separation of ilmenite and clinochlore.

3.2.2. Flotation of artificially mixed mineral

In this section, to investigate the separation performance and application of MBHA in ilmenite flotation, ilmenite and clinochlore were mixed at a mass ratio of 1:1. Based on the single mineral test results from Section 3.2.1, artificial mixed ore experiments were conducted under the optimal flotation performance conditions of MBHA and NaOL, and the results are shown in Fig. 8.

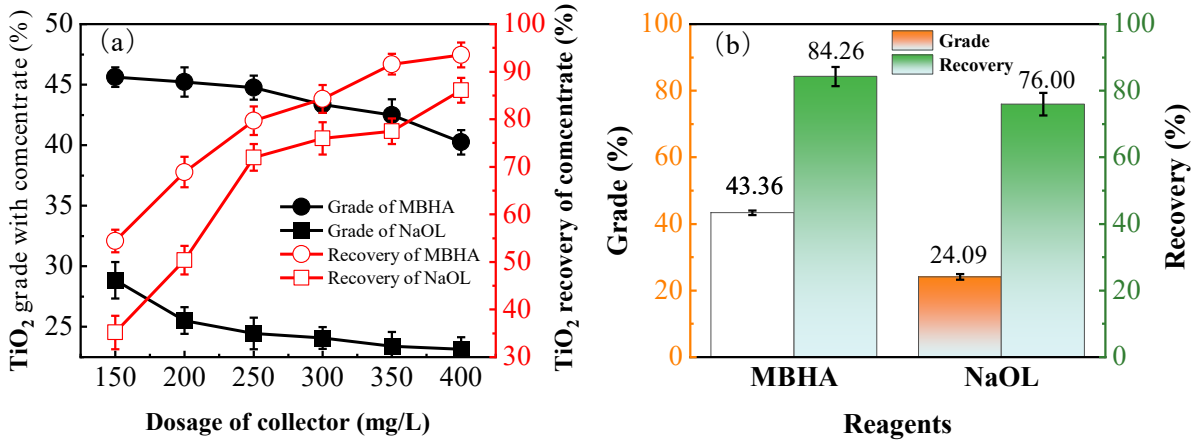

Fig. 8. (a) Effect of collector dosages on the flotation of artificially mixed minerals and (b) effect of collector concentration on the flotation concentrate with collector: 300mg/L, MBHA: pH 7.0, NaOL: pH 4.0.

As the collector dosage increases, the grade of TiO2 in the concentrate gradually decreases, while the TiO2 recovery rate gradually increases. When NaOL is used as the collector, the ilmenite grade in the concentrate is similar to the feed ore grade, making ilmenite and clinochlore difficult to separate,

whereas with the same dosage of MBHA, both the concentrate grade and recovery rate are superior to those of NaOL. When the MBHA dosage is 300 mg/L, the TiO2 grade and recovery rate in the concentrate increase from 24.09% and 76.00% (with NaOL as the collector) to 43.36% and 84.26%, respectively. When the dosage reaches 350 mg/L, the TiO2 recovery rate reaches 91.58%. The artificial mixed ore experiments further demonstrate that MBHA is a better collector than NaOL for the flotation separation of ilmenite and clinochlore.

3.3. Contact angle analysis

The floatability of minerals is closely related to their surface wettability, which can be effectively characterized by the contact angle of the minerals. This section investigates the effect of collectors on the surface wettability of ilmenite and clinochlore through contact angle measurements before and after reagent treatment, as shown in Fig. 9.

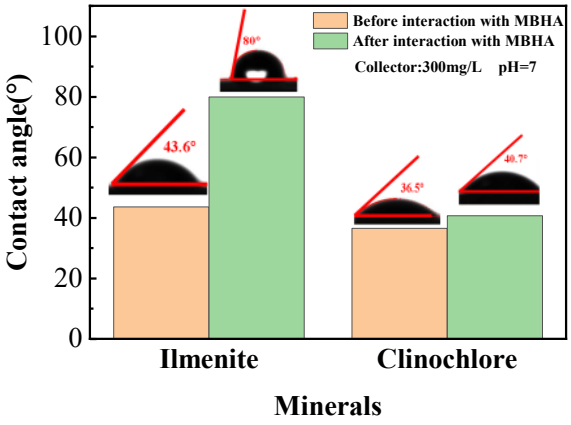

Fig. 9. Contact angle of ilmenite and clinochlore before and after interaction with MBHA

The static contact angle of raw ilmenite was approximately 43.60°, indicating its hydrophilic nature. After treatment with the collector MBHA, the surface hydrophobicity of ilmenite increased to 80.00°, indicating a significant improvement in the surface hydrophobicity of ilmenite. The contact angle of clinochlore changed from 36.50° to 40.70°. The contact angle variations of ilmenite and clinochlore were 36.40° and 4.20°, respectively, demonstrating that MBHA imparted stronger hydrophobicity to ilmenite after interaction, which is more favorable for flotation. This observation aligns with the earlier flotation results.

3.4. Zeta potential analysis

To further investigate the adsorption mechanism of the collector MBHA on the surfaces of ilmenite and clinochlore, under different pH conditions, the surface zeta potential changes of ilmenite and clinochlore before and after the addition of collector MBHA were investigated, as shown in Fig. 10.

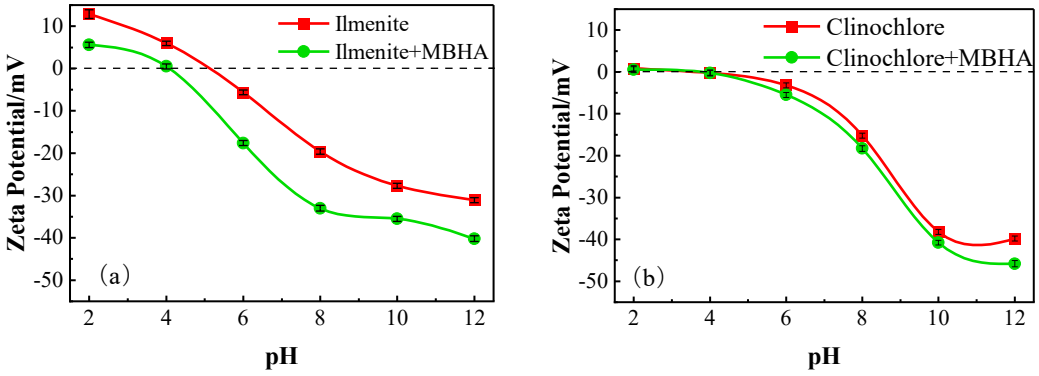

Fig. 10. Zeta potentials of (a) ilmenite and (b) clinochlore with/without MBHA at different pH values

The isoelectric point (IEP) of ilmenite is around pH=5.0, while that of clinochlore is around pH=2.0 (Niu et al., 2024; Zhang et al., 2022). The zeta potentials of both ilmenite and clinochlore decrease with increasing pH, which is consistent with previous studies (Niu et al., 2024; Zhang et al., 2022). After the addition of collector MBHA, the zeta potential of ilmenite shifts negatively across the entire pH range, indicating the adsorption of MBHA molecules on the ilmenite surface. Within the optimal flotation range for ilmenite (pH=6.0-8.0), the maximum negative shift reaches 13.40 mV. In contrast, the zeta potential of clinochlore shows negligible changes across the entire pH range after MBHA addition. These results demonstrate that MBHA exhibits strong adsorption and high adsorption capacity on the ilmenite surface, while its adsorption capability on the clinochlore surface is weak. This observation aligns with the monomineral flotation test results.

3.5. FT-IR analysis

The FTIR spectra of ilmenite and clinochlore before and after interaction with the collectors MBHA and NaOL reveal the adsorption mechanism of the collectors on the mineral surfaces, as shown in Fig. 11.

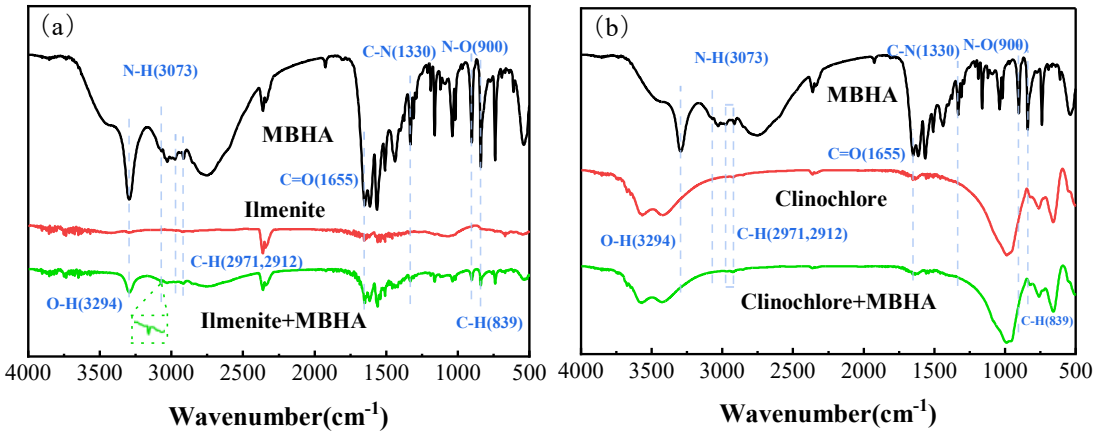

Fig. 11. Effects of MBHA on FTIR spectra of ilmenite (a) and clinochlore (b)

As shown in Fig. 11(a), the FTIR spectrum of ilmenite exhibits significant changes after MBHA treatment, with new absorption peaks emerging. In the FTIR spectrum of ilmenite interacted with the collector MBHA, the absorption peaks at 1436 cm^{-1}, 1508 cm^{-1}, 1562 cm^{-1}, and 1614 cm^{-1} correspond to the skeletal vibrations of the benzene ring, which are characteristic of aromatic structures (Luo et al., 2024). The peak at 3073 cm^{-1} is attributed to the N–H stretching vibration absorption of MBHA, while the peak at 1655 cm^{-1} corresponds to the C=O stretching vibration absorption. These observations indicate that chemical adsorption occurs between the ilmenite surface and MBHA in aqueous solution, where Ti^{4+} ions form either a five-membered "O–M–O" chelate complex or a four-membered "N–M–O" chelate complex with the nonpolar groups of MBHA (Gang et al., 2022). Furthermore, the hydrocarbon groups exhibit strong hydrophobicity, altering the surface properties of ilmenite. The adsorption is primarily through chemical adsorption, enabling ilmenite to adsorb onto air bubbles and float during flotation, with physical adsorption also contributing. In contrast, as shown in Fig. 11(b), clinochlore displays negligible spectral changes after MBHA treatment. This result further confirms that MBHA exhibits stronger adsorption on the ilmenite surface compared to clinochlore.

3.6. Adsorption heat of MBHA on ilmenite and clinochlore

To further investigate the adsorption behavior of the collector MBHA on the surfaces of ilmenite and clinochlore, the adsorption capacity patterns of MBHA with different dosages on both minerals were studied under the condition of pH=7.0, as shown in Fig. 12.

As shown in Fig. 12, MBHA adsorbs onto both ilmenite and clinochlore surfaces. However, with increasing MBHA dosage, the adsorption on ilmenite rises rapidly, reaching 0.46 mg·g^{-1} at 300 mg/L MBHA. In contrast, clinochlore adsorption increases slowly and stabilizes at 0.058 mg·g^{-1} when the dosage reaches 350 mg/L. The widening adsorption gap between the two minerals demonstrates

MBHA's significantly stronger affinity for ilmenite than clinochlore. This selective adsorption aligns with flotation results: ilmenite recovery continuously improves with higher MBHA dosage, while clinochlore recovery remains largely unaffected, further confirming MBHA's targeted collecting capability for ilmenite over clinochlore.

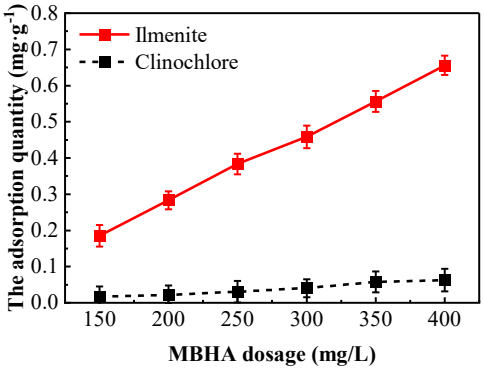

Fig. 12. Adsorption capacity of MBHA on the surface of ilmenite and clinochlore.

3.7. XPS analysis

In order to further investigate the interaction mechanisms of MBHA on the surfaces of ilmenite and clinochlore, and to further demonstrate the stronger interaction between MBHA and ilmenite compared to clinochlore, this section explores the adsorption mechanisms of MBHA on both minerals through XPS analysis. The XPS survey spectra and surface relative atomic concentration changes before and after MBHA treatment are shown in Fig. 13 and Table 2, respectively.

Table 2. The surface atomic compositions (wt.%) of ilmenite and clinochlore. (errors < ±5%)

	C	O	N	Ti	Fe	Al	Si
Ilmenite	30.12	50.31	-	7.53	5.52	-	4.56
Ilmenite+MBHA	38.03	42.71	2.50	4.43	4.28	-	4.38
Shift	7.91	-4.60	2.50	-3.10	-1.42	-	-0.18
Clinochlore	33.07	43.56	-	-	1.21	6.58	10.89
Clinochlore+MBHA	37.07	41.32	-	-	1.18	5.62	11.06
Shift	4.00	-2.24	-	-	-0.03	0.96	-0.17

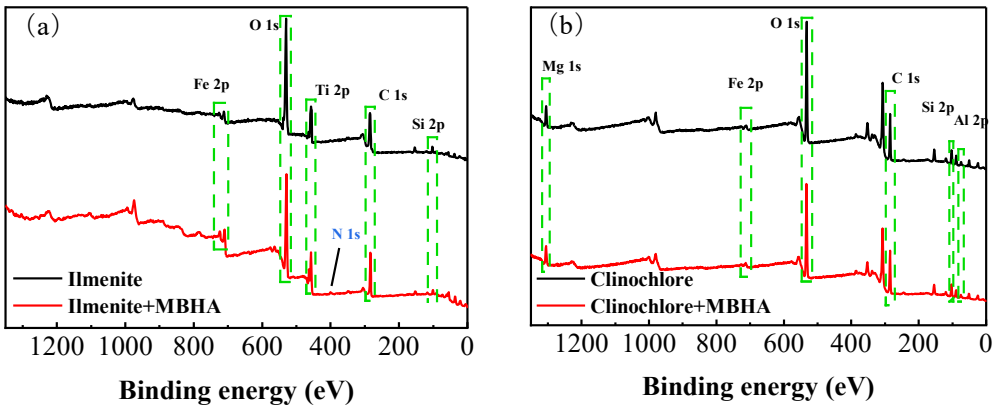

Fig. 13. XPS full spectra of ilmenite and clinochlore before and after MBHA treatment

As shown in Fig. 13(a), the characteristic atomic orbitals of ilmenite — including Ti 2p, Fe 2p, Al 2p, and Si 2p — align with its chemical composition. After MBHA treatment, a distinct N 1s peak emerged on the ilmenite surface with nitrogen content increasing to 2.53%, whereas no significant N 1s signal

was observed on clinochlore. Concurrently, the atomic concentrations of Ti and Fe on ilmenite decreased by 3.1% and 1.42%, respectively, while clinochlore exhibited negligible compositional changes. These findings collectively demonstrate selective adsorption of MBHA on ilmenite over clinochlore, with the N 1s peak attributed to the nitrogen atom in the oxime group (-RCONHOH) of MBHA.

The high-resolution N 1s and O 1s narrow-scan spectra of ilmenite and clinochlore after MBHA treatment are presented in Fig. 14.

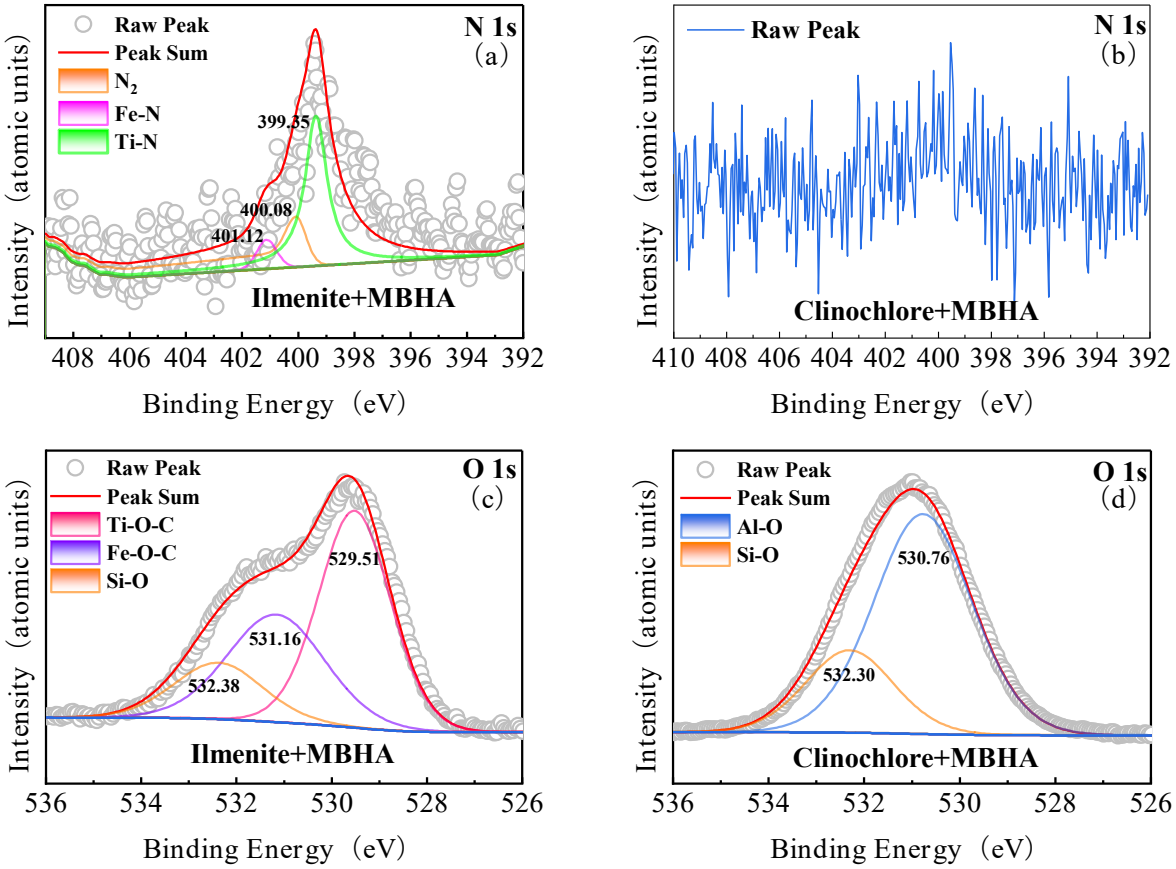

Fig. 14. High-resolution of N 1s and O 1s spectra by XPS analysis.

As shown in Fig. 14(a), the N 1s spectrum of MBHA-adsorbed ilmenite resolved into three deconvoluted peaks at 399.35 eV corresponding to Ti–N bonds, 400.08 eV assigned to neutral nitrogen species, and 401.12 eV characteristic of Fe–N bonds, which confirms the chemical adsorption of MBHA on both Ti and Fe active sites (Kang et al., 2024; Qi et al., 2024). In contrast, clinochlore displayed minimal N 1s signal intensity after MBHA treatment, as seen in Fig. 14(b), suggesting negligible or no adsorption of the reagent on its surface.

As depicted in Fig. 14(c), the O 1s spectrum of MBHA-adsorbed ilmenite was deconvoluted into three peaks: a Si–O bond signal at 532.38 eV, an Fe–O–C component at 531.16 eV, and a Ti–O–C species at 529.51 eV, confirming MBHA-induced surface coordination through both Fe and Ti oxygen bridges (Cai et al., 2020). In contrast, clinochlore treated with MBHA (Fig. 14(d)) showed only two deconvoluted peaks — a Si–O signature located at 532.30 eV and a peak at 530.76 eV assigned to Al–O bonds — indicating the absence of MBHA-derived oxygen coordination complexes (Zhang et al., 2022).

Fig. 15 and Table 3 shows the high-resolution narrow-scan spectra of the Ti 2p and Fe 2p atomic orbitals, with peak deconvolution confirming the assignments of each orbital. For ilmenite, the Ti $2p_{1/2}$ and Ti $2p_{3/2}$ orbitals correspond to binding energies of 463.36 eV and 457.69 eV, respectively (Fang et al., 2020). After interaction with MBHA, these peaks shift to 462.52 eV and 456.89 eV, indicating chemical state changes. Due to spin-orbit coupling, the Fe 2p level splits into Fe^{3+} and Fe^{2+} components (Ni and Liu, 2012; Yamashita and Hayes, 2007). The chemical shifts of Fe^{3+} for Fe $2p_{1/2}$ and Fe $2p_{3/2}$ are -0.83 eV

and -0.59 eV, respectively, while those of Fe^{2+} are -0.57 eV and -0.46 eV, suggesting that Fe^{3+} exhibits higher reactivity and preferentially binds to MBHA during chemisorption. The XPS analysis reveals that MBHA chelates with Fe and Ti sites on the ilmenite surface, forming four- and five-membered-rings, whereas its adsorption on clinochlore is negligible and dominated by electrostatic interactions. These findings align with the zeta potential and FT-IR results.

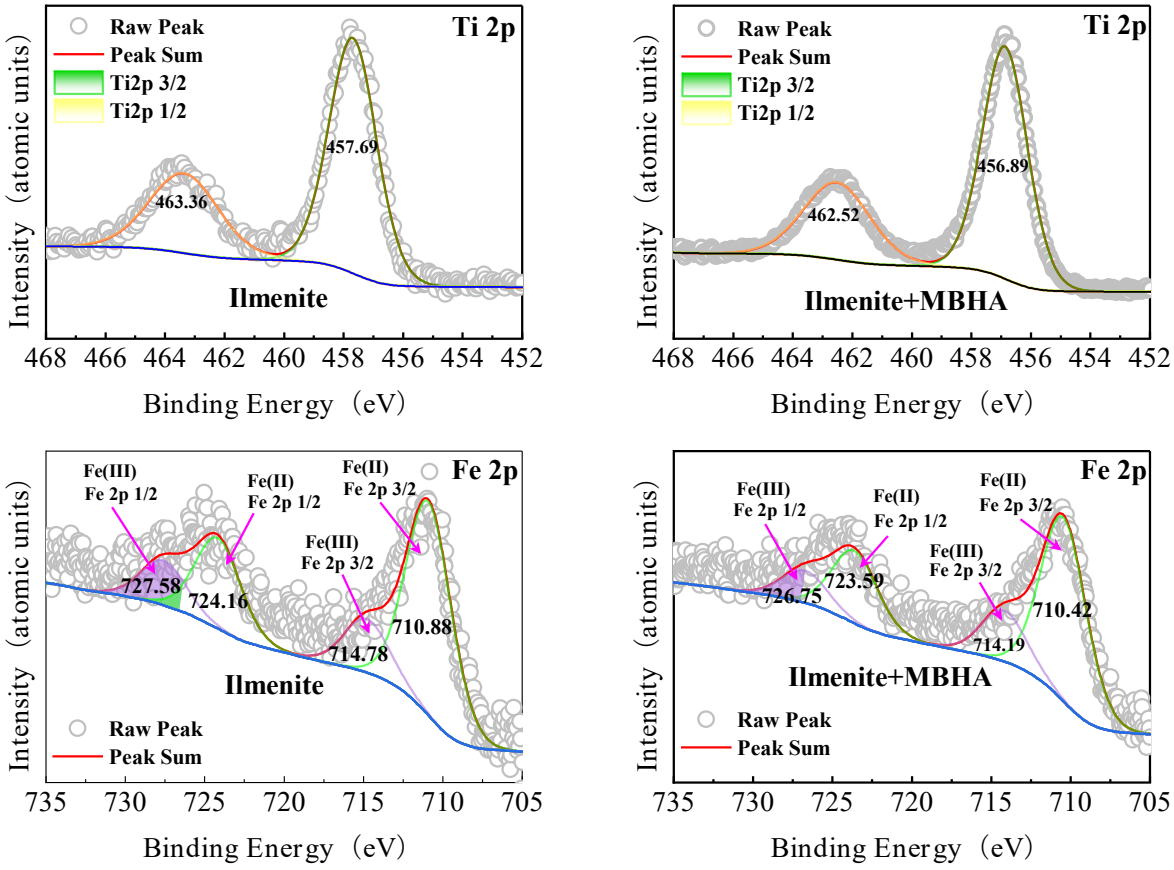

Fig. 15. High-resolution of Ti 2p and Fe 2p spectra of untreated and treated ilmenite by XPS analysis

Table 3. The change of Fe 2p, Ti 2p in binding energy of ilmenite before and after conditioning with MBHA

Atomic orbitals		Binding energy/eV		
		Ilmenite	Ilmenite+MBHA	Shift
Ti 2p	Ti $2p_{1/2}$	463.36	462.52	-0.84
	Ti $2p_{3/2}$	457.69	456.89	-0.8
Fe 2p	Fe $2p_{1/2}$ Fe^{2+}	724.16	723.59	-0.57
	Fe $2p_{1/2}$ Fe^{3+}	727.58	726.75	-0.83
	Fe $2p_{3/2}$ Fe^{2+}	710.88	710.42	-0.46
	Fe $2p_{3/2}$ Fe^{3+}	714.78	714.19	-0.59

3.8. Interaction model of MBHA on mineral surfaces

Through zeta potential analysis and various analytical methods, the adsorption model of MBHA on the ilmenite surface has been established. The adsorption model is shown in Fig. 16. Through Zeta potential and XPS analyses, it is found that after the collector MBHA is added, MBHA molecules are adsorbed on the surface of ilmenite. The Zeta potential of ilmenite shifts negatively over the entire pH range, and Fe^{2+}, Fe^{3+}, Ti^{4+}, etc. on the surface of ilmenite interact with MBHA. Moreover, based on the chemical shifts of Fe^{3+} and Fe^{2+} in Fe $2p_{1/2}$ and Fe $2p_{3/2}$, it can be known that during the chemical adsorption between ilmenite and MBHA, Fe^{3+} is more active and preferentially combines with MBHA. These substances form chemical bonds with MBHA, resulting in various five-membered-ring chelates as

shown in Figure 16. Combining XPS analysis, Zeta analysis, and FT-IR analysis, it can be confirmed that MBHA undergoes strong chemical adsorption on the surface of ilmenite.

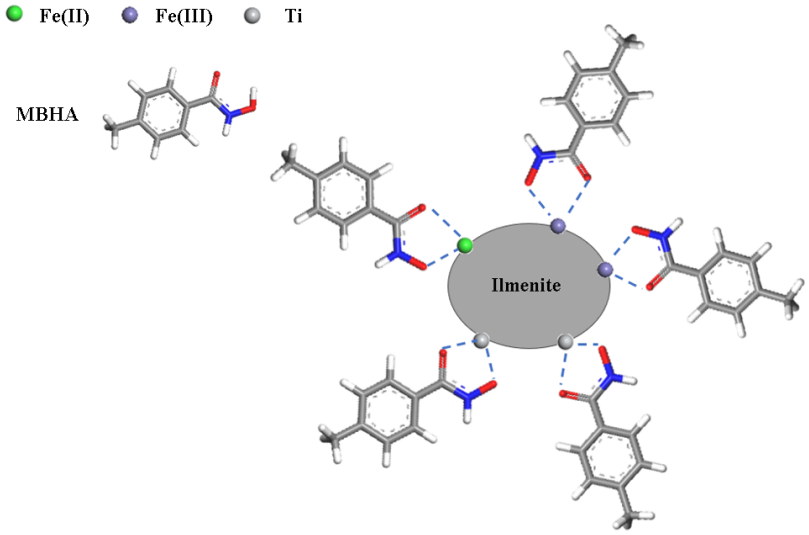

Fig. 16. Adsorption model of MBHA on ilmenite surface

4. Conclusions

This study successfully synthesized a novel hydroxamic acid-based collector, MBHA, and applied it to the flotation separation of ilmenite and clinochlore. The collecting capability and selectivity of MBHA were systematically investigated through flotation experiments, with comparative analyses against NaOL. The selective adsorption mechanism of MBHA was further elucidated via adsorption capacity measurements, FT-IR spectroscopy, zeta potential analysis, contact angle measurements, and XPS. The main conclusions are summarized as follows:

(1) Flotation experiments demonstrated that MBHA exhibits superior collecting capability and selectivity compared to NaOL. Under their respective optimal conditions, when treating an artificially blended 1:1 mixture of ilmenite and clinochlore, the concentrate TiO_2 grade increased from 24.09% (with NaOL) to 43.36%, while the recovery rate improved from 75.99% to 84.26% when MBHA was employed as the collector.

(2) MBHA predominantly adsorbs onto the ilmenite surface via chemisorption, significantly increasing its static contact angle from 43.60° to 80.00°, whereas it exhibits weak physisorption on clinochlore, with the contact angle rising only marginally from 36.50° to 40.70°.

(3) Zeta potential, FTIR, and XPS analyses revealed that MBHA undergoes strong chelation adsorption with Ti and Fe sites on the ilmenite surface, forming four- and five-membered coordination rings, whereas its adsorption on clinochlore is primarily electrostatic and significantly weaker compared to that on ilmenite.

Acknowledgments

This research was funded by the National Natural Science Foundation of China (No. 52374265), the Central Guided Local Science and Technology Development Funding Program (No. 236Z4106G), the Open Foundation of State Environment Protection Key Laboratory of Mineral Metallurgical Resources Utilization and Polution Control (HB202305).

References

BAI, R., ZHAO, F., LIU, C., *Selective flotation separation of bastnaesite from calcite using p-methyl/methoxy benzohydroxamic acid collectors.* Journal of Industrial and Engineering Chemistry, 2025, 143, 283-292.

CAI, J., DENG, J., WEN, S., ZHANG, Y., WU, D., LUO, H., CHENG, G., *Surface modification and flotation improvement of ilmenite by using sodium hypochlorite as oxidant and activator.* Journal of Materials Research and Technology, 2020, 9(prepublish), 3368-3377.

CHENG, C., ZENG, G., HUANG, J., *Benzohydroxamic acid derivatives: Structure-activity relationships in the malachite flotation.* Separation and Purification Technology, 2025, 360(P1), 130923-130923.

FAN, G., WATERS, K.E., ROWSON, N.A., PARKER, D.J., *Modification of ilmenite surface chemistry for enhancing surfactants adsorption and bubble attachment.* Journal of Colloid And Interface Science, 2008, 329(1), 167-172.

FANG, S., XU, L., WU, H., TIAN, J., LU, Z., SUN, W., HU, Y., *Adsorption of Pb(II)/benzohydroxamic acid collector complexes for ilmenite flotation.* Minerals Engineering, 2018, 126, 16-23.

FANG, S., XU, L., WU, H., XU, Y., WANG, Z., SHU, K., HU, Y., *Influence of surface dissolution on sodium oleate adsorption on ilmenite and its gangue minerals by ultrasonic treatment.* Applied Surface Science, 2020, 500, 144038-144038.

HONG, G., NAM, H., MWEENE, L., KIM, H., *Mitigation strategies of salicylhydroxamic acid collector with oxalic acid in goethite flotation.* Inorganic Chemistry Communications, 2025, 171, 113528-113528.

KANG, Y., ZHANG, C., WANG, H., XU, L., LI, P., LI, J., LI, G., PENG, W., ZHANG, F., FAN, G., CAO, Y., *A novel sodium trans-2-nonene hydroxamate for the flotation separation of ilmenite and forsterite: Superior collecting and selectivity.* Separation and Purification Technology, 2024, 333.

KUIXIN, C., SHENGMING, J., NAN, D., *Insights into the adsorption mechanism of benzohydroxamic acid in the flotation of rhodochrosite with Pb^{2+} activation.* Powder Technology, 2023, 427.

LIU, C., GAO, P., LIU, C., GUO, C., WEN, G., *Flotation performance and adsorption mechanism of monazite after the transformation of hydrogen-based mineral phase by octyl hydroxamic acid.* Powder Technology, 2025a, 451, 120462-120462.

LIU, C., KANG, J., ZHANG, B., SUN, W., TIAN, G., *The synthesis of a novel flotation collector for bastnaesite, 5,5'-methylenedisalicylic acid, based on salicylhydroxamic acid molecular structure.* Minerals Engineering, 2025b, 222, 109147-109147.

LIU, R., YANG, Z., LI, J., CAO, Z., LI, Q., *The influence of metal ions on the adsorption of octyl hydroxamic acid in the flotation of bastnaesite and the adsorption mechanism.* Physicochemical Problems of Mineral Processing, 2024.

LUO, Y., SUN, W., HE, J., PENG, J., JIANG, F., *Innovative discovery on the impact of hydration on the alternative flotation of smithsonite and calcite under benzohydroxamic acid system.* Journal of Molecular Liquids, 2024, 415(PB), 126433-126433.

MEHDILO, A., IRANNAJAD, M., REZAI, B., *Effect of crystal chemistry and surface properties on ilmenite flotation behavior.* International Journal of Mineral Processing, 2015, 137, 71-81.

NI, X., LIU, Q., *The adsorption and configuration of octyl hydroxamic acid on pyrochlore and calcite.* Colloids and Surfaces A: Physicochemical and Engineering Aspects, 2012, 411, 80-86.

NIU, F., CHEN, Y., ZHANG, J., LIU, F., WANG, Z., *Selective flocculation-flotation of ultrafine hematite from clay minerals under asynchronous flocculation regulation.* International Journal of Mining Science and Technology, 2024, 34(11), 1563-1574.

PENG, J., ZHENG, Y., WANG, Z., DAI, Z., GUO, Z., *Study on the surface activation of ilmenite by persulfate and flotation response.* Separation and Purification Technology, 2024, 343, 127079-.

QI, J., TU, J., TONG, X., XIE, R., *Flotation enrichment of ilmenite in oxidation system with a short-chain dithiocarbamate-hydroxamate collector.* Applied Surface Science, 2025, 694, 162855-162855.

QI, J., XIE, X., TONG, X., *Highly efficient flotation of ilmenite with a novel dithiocarbamate-hydroxamate collector.* Applied Surface Science, 2024, 669.

WANG, Y., WANG, D., XU, L., XUE, K., ZHANG, X., SHI, X., LIU, C., MENG, J., Synthesis and utilization of a novel oleate hydroxamic acid collector for the flotation separation of bastnaesite from barite. Minerals Engineering, 2023, 204.

XIAO, W., SHAO, Y., YU, J., ZHANG, B., SHU, H., ZHANG, Y., *Activation of ilmenite flotation by Al^{3+} in the benzohydroxamic acid (BHA) system.* Separation and Purification Technology, 2022, 299.

YADAV, G.D., KATOLE, S.O., *Synthesis of green bioadditives via esterification of glycerol with acetic acid catalysed by modified heteropolyacid on clay support.* Journal of the Indian Chemical Society, 2025, 102(4), 101623-101623.

YAMASHITA, T., HAYES, P., *Analysis of XPS spectra of Fe^{2+} and Fe^{3+} ions in oxide materials.* Applied Surface Science, 2007, 254(8), 2441-2449.

YU, J., PENG, L., ZHANG, B., ZOU, J., HU, Y., JI, Y., YANG, C., YU, J., *Rutile-quartz separation in benzohydroxamic acid and sodium oleate flotation systems.* Next Materials, 2025a, 8, 100525-100525.

YU, J., ZHAO, F., CHEN, B., YE, Z., LIU, C., LIU, C., ZENG, H., *Enhanced fluorite-calcite separation through selective hydroximic acid adsorption driven by cationic-π interactions.* Chemical Engineering Journal, 2025b, 509, 161162-161162.

ZHANG, C., LI, P., CAO, Y., HAO, H., PENG, W., TENG, D., FAN, G., *Synthesis of sodium oleate hydroxamate and its application as a novel flotation collector on the ilmenite-forsterite separation.* Separation and Purification Technology, 2022, 284.

ZHANG, X., LIU, D., FANG, J., XU, J., *Study on Influence of Residual Magnetite in Panzhihua Ilmenite Flotation.* Procedia Earth and Planetary Science, 2011, 2, 83-88.

ZHAO, G., ZHONG, H., QIU, X., WANG, S., GAO, Y., DAI, Z., HUANG, J., LIU, G., *The DFT study of cyclohexyl hydroxamic acid as a collector in scheelite flotation.* Minerals Engineering, 2013, 49, 54-60.

ZHAO, Z., XIE, R., WANG, X., TONG, X., XIE, X., ZHOU, W., *Study on flotation separation of chlorite and kaolinite by modified fatty acid collector and its mechanism.* Colloids and Surfaces A: Physicochemical and Engineering Aspects, 2025, 704, 135510-135510.

ZHU, Y.-G., ZHANG, G.-F., FENG, Q.-M., YAN, D.-C., WANG, W.-Q., *Effect of surface dissolution on flotation separation of fine ilmenite from titanaugite.* Transactions of Nonferrous Metals Society of China, 2011, 21(5), 1149-1154.